A PRIORI ASSESSMENT OF ALGEBRAIC AND DIFFERENTIAL REYNOLDS-STRESS MODELS USING DNS DATABASE

J. Knoell and S. Jakirlić
Fachgebiet Strömungslehre und Aerodynamik, Darmstadt University of Technology,
Petersenstrasse 30, 64287 Darmstadt, Germany
K. Hanjalić
Faculty of Applied Physics, Delft University of Technology,
Lorentzweg 1, 2628 CJ Delft, The Netherlands

ABSTRACT

We performed a comparative *a priori* examination of several *algebraic and differential second-moment closure models* (ASM and DSM) using the DNS database for three generic flows: fully developed channel flow (Moser et al., 1999), flow in an axially rotating pipe (Eggels et al., 1994 and Orlandi and Ebstein, 1999) and the flow over a backward-facing step (Le et al., 1997). First, the coefficient functions $G^{(i)}$ and the basis tensors in the algebraic expression for the Reynolds-stress tensor, as well as the stress components themselves, were evaluated and compared for several ASMs. Then, the model coefficients of the pressure-strain term in the DSM were deduced from the DNS database, and compared with different model proposals. Last, the term-by-term analysis of the pressure-strain and dissipation correlation for several DSMs were performed.

INTRODUCTION

Rampant number of different model suggestions for turbulence closures and consequent confusion among potential users call for a further comparative scrutiny of the various model proposals in a broader number of generic flows with different features. This analysis focuses on two separate - though related, issues, each representing the backbone and major target of model improvement in the two model classes considered. The first part deals with the nonlinear stress-strain relations, which are either based on implicit algebraic stress models or are formal higher order extensions to the linear model proposal relating the Reynolds stresses to the mean velocity field. The second part focuses on differential Reynolds stress models and here on the model for the pressure-strain and dissipation correlations as the crucial unknown terms.

ALGEBRAIC STRESS MODELS

Most recent proposals for improving eddy-viscosity two-equation models use a higher order nonlinear constitutive stress-strain relationship. Following the conjecture that the Reynolds stress anisotropies $a_{ij} = \overline{u_i u_j}/k - 2\delta_{ij}/3$ are uniquely determined by the mean velocity field and local scalar turbulence scales, defined in terms of the turbulent kinetic energy k and its dissipation rate ϵ (or a combination of these two variables), allows to generate a closed set of equations for a_{ij}. For the general three-dimensional case the Cayley-Hamilton theorem yields the most general relationship for the stress anisotropy tensor in terms of five independent basis tensors $T_{ij}^{(n)}$ consisting of various traceless combinations of the mean rate of strain S_{ij} and the mean rate of rotation Ω_{ij}.

$$a_{ij} = \sum_{n=1}^{5} G^{(n)} T_{ij}^{(n)} \tag{1}$$

Pope (1975) originally suggested to use ten independent basis tensors in the above expression, with the coefficients expressed as rational polynomials of the invariants resulting from the various combinations of S_{ij} and Ω_{ij}. According to Rivlin and Ericksen (1955) however, there can only be five independent symmetric and traceless 3×3 tensors. Therefore, if a less restrictive formulation of $G^{(n)}$ is assumed, a 5-tensor basis is sufficient. Confining the attention to two-dimensional flows for the following analysis results in a nonlinear stress-strain relation that can be written as a combination of three independent basis tensors:

$$\begin{aligned} a_{ij} &= G^{(1)} \overbrace{S_{ij}}^{T_{ij}^{(1)}} + G^{(2)} \overbrace{(S_{ik}S_{kj} - \frac{1}{3} S_{kl}S_{lk}\delta_{ij})}^{T_{ij}^{(2)}} \\ &+ G^{(3)} \underbrace{(S_{ik}\Omega_{kj} - \Omega_{ik}S_{kj})}_{T_{ij}^{(3)}} \end{aligned} \tag{2}$$

where $S_{ij} = (\partial U_i/\partial x_j + \partial U_j/\partial x_i)/2$ and $\Omega_{ij} = (\partial U_i/\partial x_j - \partial U_j/\partial x_i)/2$.

In two-dimensional flows the coefficients $G^{(i)}$ can be functions of only two independent invariants $S_{kl}S_{lk}$ and $\Omega_{kl}\Omega_{lk}$, of the scale providing quantities k and ϵ, and of various model parameters. One way to determine the proper form of the coefficients $G^{(i)}$ is to solve a simplified version of the differential Reynolds stress transport equation as suggested by Pope (1975). If both the transport and the convective term are abandonned the partial differential equation for a_{ij} can be transformed into an algebraic equation allowing for a solution if the appropriate ansatz of Eq. (2) is chosen. The advantage is that now all model parameters in the nonlinear stress-strain relation are determined by the model parameters of the pressure-strain correlation of the underlying differential Reynolds stress model. The other way to determine $G^{(i)}$ is to systematically extend the linear stress-strain relation utilized in the standard $k-\epsilon$ model. Depending on the model formulation, the coefficient functions can differ significantly. In all cases, however, the scale providing quantities influencing the nonlinear stress-strain relation can be determined via a k-ϵ model.

In this paper six different nonlinear stress-strain relations based on the works by Craft *et al.* (CLS, 1996), Jongen *et al.* (JMG, 1998), Khodak and Hirsch (KH, 1996), Knoell and Taulbee (KT, 1999) and Wallin and Johansson (WJ, 2000) are assessed in an a priori manner by expressing the specific model formulation in a way consistent with Eq. (2) and then inserting DNS data for k, ϵ and the mean velocity field to compute the components of a_{ij}. This procedure has the advantage that any contamination of the expression for $\overline{u_i u_j}$ due to inaccuracies in the modeled transport equation for k and ϵ and vice versa is avoided. It is believed that these contaminations, that may become invisible in the final computational results when the complete model is used due to compensating errors, are not negligible and reduce the applicability of turbulence models to only a limited family of flows in which the model was tuned.

Two examples of this assessment, Figs. 1, show the results for the first two normal stresses and the shear stress in the boundary layer upstream from a backward facing step at the position $x/H = -3$. Apart from some details in the near-wall region, all models considered agree fairly well with the DNS data. Furthermore, using the DNS data the correct behavior of the coefficient functions $G^{(i)}$ and the basis tensors can be deduced as follows: inserting the available DNS data for the mean velocity field and the Reynolds stress anisotropies results in a linear 3×3 system of equations for $G^{(i)}$, which can be solved to determine $G^{(i)}$ directly from DNS data. Now it is possible to compare the model formulations for each of the three terms in the ansatz for a_{ij} with the corresponding data from the DNS as shown in Figs. 2 for $G^{(1)}T^{(1)}_{11}$, $G^{(2)}T^{(2)}_{11}$ and $G^{(1)}T^{(1)}_{12}$. The overall agreement is reasonable considering the very complex nature of the functionality.

a)

b)

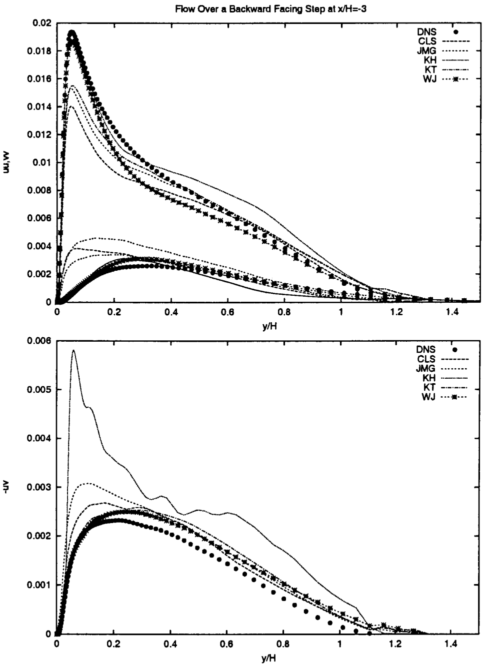

Fig. 1. Boundary layer upstream from a backward-facing step flow: a) $\overline{u^2}$, $\overline{v^2}$ and b) $\overline{uv}$ stress components at the position $x/H = -3$

a)

b)

c)

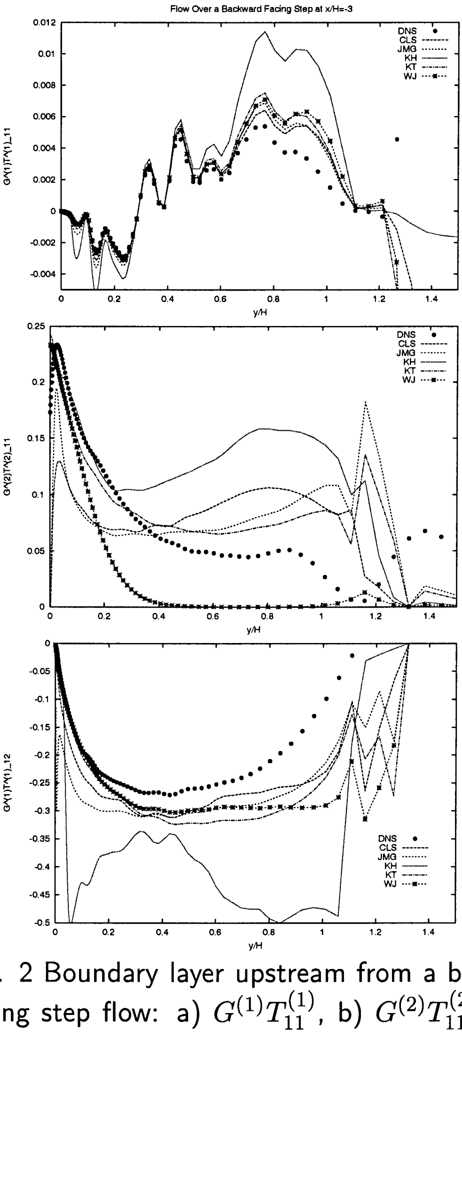

Fig. 2 Boundary layer upstream from a backward-facing step flow: a) $G^{(1)}T^{(1)}_{11}$, b) $G^{(2)}T^{(2)}_{11}$ and c)

$G^{(1)}T_{12}^{(1)}$ products at the position $x/H = -3$

In the outer region of the boundary layer the three building blocks of the constitutive equation show some random behavior. Here the results are strongly affected by the noise in the DNS data for k and ϵ. With the help of this methodology the three terms in Eq. (2) can independently be assessed allowing a very effective way of calibrating the model parameters. Fig. 3 illustrates the a priori behavior of the two normal Reynolds stresses and the shear stress at the station within the recirculating region in a backstep flow ($x/H = 4$). Again, the overall agreement is fair except from some inconsistencies stemming from the near-wall formulation. Here the new approach can be very useful for a re-evaluation of the critical wall modifications.

a)

b)

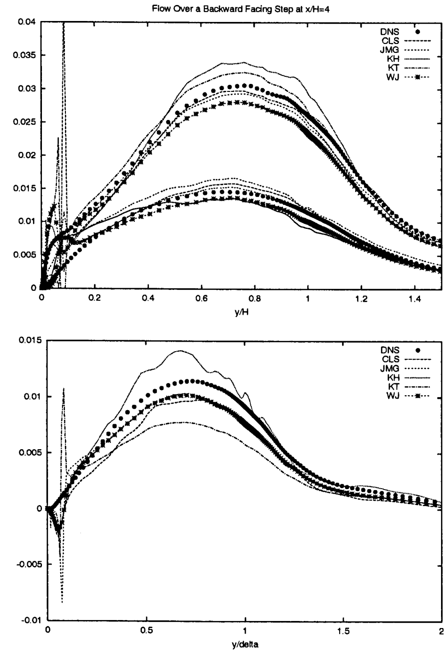

Fig. 3. Backward-facing step flow: a) $\overline{u^2}$, $\overline{v^2}$ and b) $\overline{uv}$ stress components at the position $x/H = 4$ within the separation bubble

Furthermore, the peaks in the *a priori* predictions of the stresses can now clearly be attributed to the domination of the denominator in the coefficients $G^{(n)}$ approaching zero and thus creating singularities. This effect can be avoided by a regularization procedure on the basis of a Padé approximation, as discussed by Gatski and Speziale (1993). However, this approximation can be considered as an ad-hoc modification not originating from the exact solution of the reduced Reynolds-stress transport equation.

DIFFERENTIAL STRESS MODELS

The key issues in closing the transport equations for the turbulent Reynolds stresses are the modelling of the pressure scrambling process, viscous destruction - dissipation, and turbulent transport. An analysis of behaviour of several, most frequently used model schemes of the two former processes will be given here, using DNS results for the three generic flows mentioned earlier.

Pressure-strain models

All model proposals for the slow (see, e.g., Speziale et al., 1991) and rapid (see, e.g., Johansson and Hallbäck, 1994) parts of the pressure-strain correlation in the differential second-moment closures can be written in general forms, respectively:

$$\Phi_{ij,1} = -\varepsilon \left[C_1 a_{ij} + C_1' \left(a_{ik}a_{kj} - \frac{1}{3}A_2\delta_{ij} \right) \right] \quad (3)$$

$$\begin{aligned}
\frac{\Phi_{ij,2}}{k} &= Q_1 S_{ij} + \\
&Q_2 \left(a_{ip}S_{pj} + a_{jp}S_{pi} - \frac{2}{3}a_{pq}S_{pq}\delta_{ij} \right) + \\
&Q_3 a_{ij}a_{pq}S_{pq} + \\
&Q_4 \left(a_{iq}a_{jp} - \frac{1}{3}a_{pk}a_{kq}\delta_{ij} \right) S_{pq} + \\
&Q_5 \left[a_{pl}a_{lq}a_{ij} + a_{pq} \left(a_{ik}a_{kj} - \frac{1}{3}A_2\delta_{ij} \right) \right] S_{pq} + \\
&Q_6 a_{pl}a_{lq} \left(a_{ik}a_{kj} - \frac{1}{3}A_2\delta_{ij} \right) S_{pq} + \\
&Q_7 \left(a_{ip}\Omega_{pj} + a_{jp}\Omega_{pi} \right) + \\
&Q_8 a_{pk}(a_{jk}\Omega_{pi} + a_{ik}\Omega_{pj}) + \\
&Q_9 a_{pk}(a_{jk}a_{iq} + a_{ik}a_{jq})\Omega_{pq} \quad (4)
\end{aligned}$$

The scalar functions C_1 and C_1' as well as Q_{1-9}, all written in terms of the second ($A_2 = a_{ij}a_{ji}$) and third ($A_3 = a_{ij}a_{jk}a_{ki}$) invariants of a_{ij} and turbulence Reynolds-number $Re_t = k^2/(\nu\varepsilon)$ are determined applying different mathematical constraints such as the symmetry in indices, continuity, Green's condition, realizibility, as well as the principles of material frame indifference. In addition, some homogeneous flows and the rapid distortion theory are used for the calibration of the coefficients.

We consider in parallel the following models: the linear model by Launder et al. (LRR, 1975) and Gibson and Launder (GL, 1978) quadratic by Shih and Lumley (SL, 1985) and Speziale et al.(SSG, 1991), cubic by Fu et al. (FLT, 1987), Launder and Li (LL, 1994) and Ristorcelli et al. (RLA, 1995,) and the 4-th order model by Johansson and Hallbäck, (JH, 1994). In addition, considered are also the low-Re-number extensions of the basic Reynolds-stress model by Hanjalic and Jakirlic (HJ, 1998), by Launder and Tselepidakis (LT, 1993) and Craft et al. (CKL, 2001) i.e. Craft (1998). Because of space limitation, the coefficients will be not listed here. The readers can consult the references mentioned above.

The most general model for the slow part is quadratic, because the Cayley-Hamilton theorem allows higher powers of a_{ij} to be expressed in terms of a_{ij} and a_{ij}^2. This quadratic model can be written as in equation (3), where the profiles of coefficients C_1 and C_1' take different shapes for different model formulations, Fig. 4. The DNS database for fully developed channel flow (the only DNS where the slow and rapid parts are evaluated separately, Mansour et al., 1988) enables the evaluation of the profiles of the model coefficients C_1 and C_1'. For each combination of two different components of the slow part $\Phi_{ij,1}$, equation (3) can be written as a system of two equations with two unknowns: C_1 and C_1'. For, e.g., $ij = 11$ and $ij = 22$ this equations system reads:

$$a_{11}C_1 + \left(a_{11}^2 + a_{12}^2 - \frac{1}{3}A_2\right) C_1' = -\Phi_{11,1}/\varepsilon$$

$$a_{22}C_1 + \left(a_{12}^2 + a_{22}^2 - \frac{1}{3}A_2\right) C_1' = -\Phi_{22,1}/\varepsilon$$

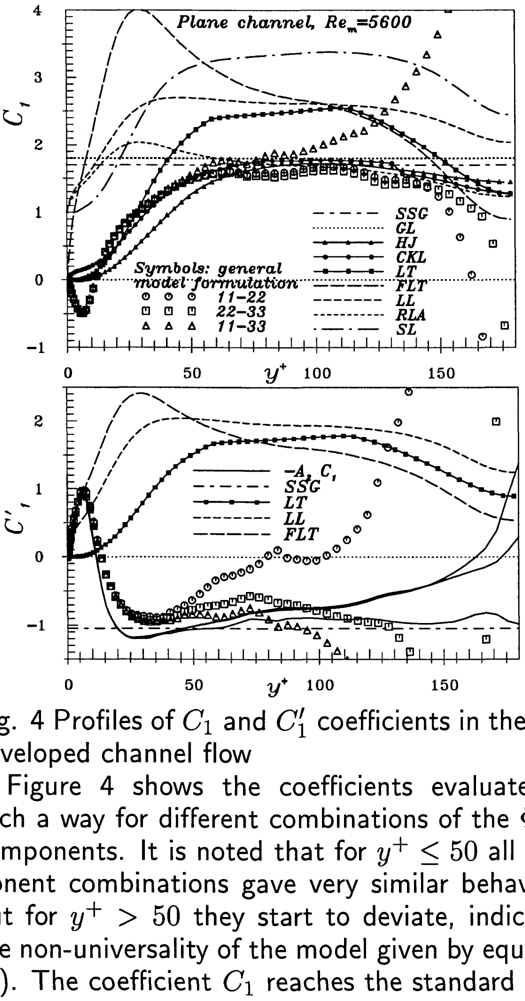

Fig. 4 Profiles of C_1 and C_1' coefficients in the fully developed channel flow

Figure 4 shows the coefficients evaluated in such a way for different combinations of the $\Phi_{ij,1}$-components. It is noted that for $y^+ \leq 50$ all component combinations gave very similar behaviour, but for $y^+ > 50$ they start to deviate, indicating the non-universality of the model given by equation (3). The coefficient C_1 reaches the standard high-Reynolds number value $1.7-1.8$ away from the wall, in a good agreement with the most of the model proposals. Several low-Reynolds number models analysed (CKL, LT and HJ) show reasonable agreement with DNS result for C_1 over the whole flow, especially the Craft et al. (2000) model, although none of the models captures the sign change in C_1 in the immediate wall vicinity, for $y^+ < 10$. The Shih and Lumley model of the C_1 coefficient results in a significant overprediction (up to 3.5), which is the main reason for large deviations obtained with this model when performing the term-by-term comparison, Figs. 5-7. The evaluated coefficient C_1' is negative, apart from very close to the wall, showing in fact an opposite behaviour from C_1. A good approximation is $C_1' = -A_2C_1$ (the full lines in Fig. 4b). Far from a wall the value of C_1' is close to that proposed by Speziale et al. (SSG, 1991), $C_1' = -1.05$, at least in the logarithmic region. This is opposite from the model formulations proposed by FLT, LT and LL, all resulting in a large positive value. This deviation is obviously compensated by the model of the rapid part, in view of good agreement with DNS when the complete pressure strain term Φ_{ij} is considered, Figs. 5-7. We obtained similar behaviour by evaluating the coefficients C_1 and C_1' from the entire term, using the model of the pressure redistribution as a whole (slow part + rapid part). We also performed similar evaluation of the coefficients in the rapid part, but only for the linear model with three unknown coefficients (not shown here).

The direct comparison of the models of the pressure-strain redistribution in *term-by-term* manner is shown in Fig. 5 for the fully developed channel flow and in Figs. 6 and 7 for the flow over a backward-facing step.

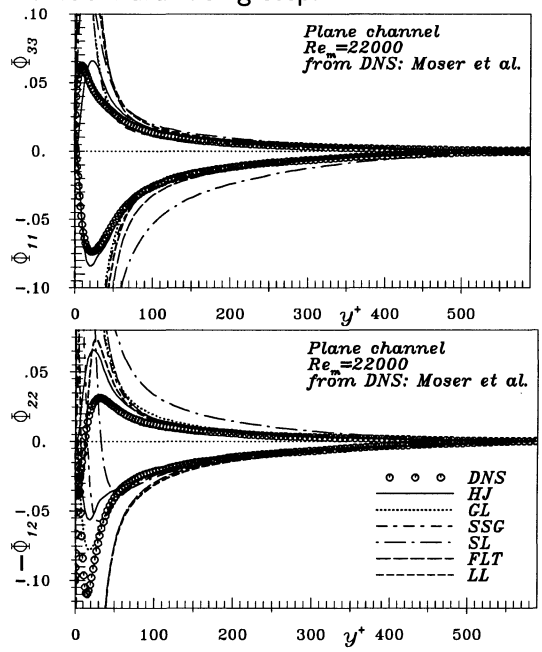

Fig. 5 Models evaluation of the pressure-strain term in the fully developed channel flow

Two locations along the step-wall were selected: $x/H = 4$ which is in the recirculation zone whose length is about $x_R/H = 6.28$, and $x/H = 19$ corresponding to the "new" (recovering) boundary layer, but still far from equilibrium (note the modified Φ_{ij}-profile compared with the channel flow). All models predict the general shape of the term Φ_{ij} fairly well for both flows. With exception of the SL model, all model results follow the DNS data fairly close. As already mentioned, the large value of the C_1 coefficient in the SL model causes almost the complete deviation between model results and DNS. The only low-Reynolds model tested here, the HJ model, does not reproduce the change in sign of all four components of the Φ_{ij} close to the wall in the separation bubble. The performances of the JH model, which is the only model of the fourth order, was not analyzed here, because it does not have a corresponding slow part being necessary for prediction of the entire Φ_{ij}.

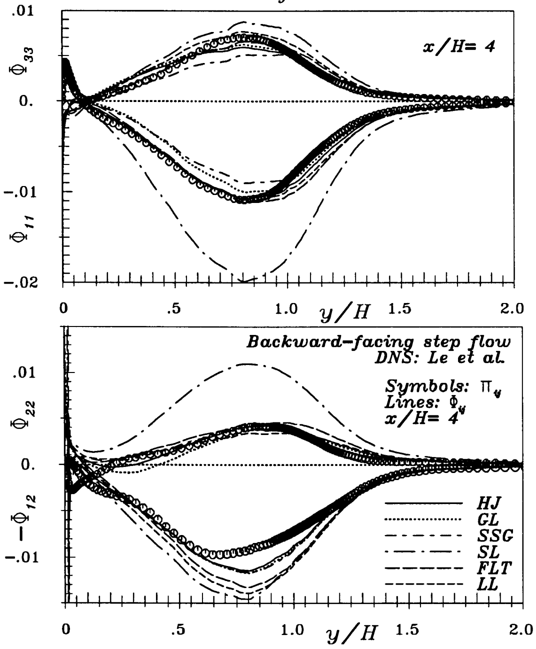

Fig. 6 Pressure-strain term in the recirculation zone $(x/H = 4)$ behind a backward-facing step

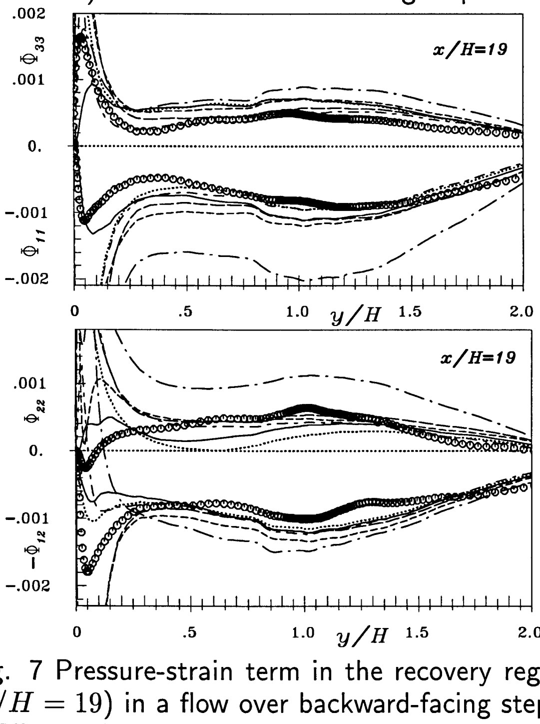

Fig. 7 Pressure-strain term in the recovery region $(x/H = 19)$ in a flow over backward-facing step

The evaluation of these models by integrating numerically the transport equations for the turbulent stresses, using the DNS results for the mean velocity and dissipation rate fields, as well as some terms in the $\overline{u_iu_j}$-budgets: turbulent transport term and dissipation correlation, is in progress.

Dissipation correlation

The most widely used model for the dissipation tensor ε_{ij} is based on the assumed proportionality between the small scale anisotropy - represented by the deviatoric of the dissipation rate tensor $e_{ij} = \varepsilon_{ij}/\varepsilon - 2/3\delta_{ij}$, and the large scale anisotropy represented by a_{ij} (Hanjalic and Launder, 1976). Using this formulation for the homogeneous part of the dissipation correlation and adding its nonhomogeneous part, which is exactly defined as the half of the molecular diffusion of the corresponding turbulent stresses (Jovanovic et al., 1995), the following algebraic relationship for ε_{ij} is obtained:

$$\varepsilon_{ij} = (1 - f_s)\frac{2}{3}\delta_{ij}\varepsilon^h + f_s\frac{\overline{u_iu_j}}{k}\varepsilon^h + \frac{1}{2}\mathcal{D}^{\nu}_{ij} \qquad (5)$$

where f_s is the blending function which should provide transition from the low-Re-number and wall limit $(\overline{u_iu_j}\varepsilon/k)$ and the high-Reynolds-number limit $(2/3\varepsilon\delta_{ij})$. From the models of this kind, Jakirlic and Hanjalic model (HJ, 2001) with $f_s = 1 - \sqrt{A}E^2$ (A and E stand for the two-componentality factors of the stress and dissipation anisotropies respectively) was compared with the Hallbäck *et al.* model (HGJ, 1990) and the DNS data for the backward-facing step flow and the flow in an axially rotating pipe. Hallbäck *et al.* model represents a second order formulation as follows:

$$e_{ij} = \left[1 + \alpha\left(\frac{1}{2}A_2 - \frac{2}{3}\right)\right]a_{ij} - \alpha\left(a_{ik}a_{kj} - \frac{1}{3}A_2\delta_{ij}\right) \qquad (6)$$

This model is developed for homogeneous flows, meaning that the dissipation rate ε represents actually the homogeneous dissipation. We have modified the above HGJ expression by adding the nonhomogeneous part of the dissipation correlation to account for the near wall effects, denoted as HGJ-M model:

$$\begin{aligned}\varepsilon_{ij} &= (1 - f_s)\frac{2}{3}\delta_{ij}\varepsilon^h + f_s\frac{\overline{u_iu_j}}{k}\varepsilon^h - \\ &\quad \alpha\varepsilon^h\left(a_{ik}a_{kj} - \frac{1}{3}A_2\delta_{ij}\right) + \frac{1}{2}\mathcal{D}^{\nu}_{ij} \qquad (7)\end{aligned}$$

where $f_s = 1 + \alpha(A_2/2 - 2/3)$, $\alpha = 3/4$.

These two model formulations are compared in the following figures. The Rotta's isotropic, high-Reynolds proposal $(2/3\varepsilon\delta_{ij})$ is also shown.

Fig. 8 shows the ε_{11}, ε_{33} and ε_{13} components of the dissipation correlation in the axially rotating pipe flow for a weak rotation rate $(N = 0.61)$, being close to the non-rotating case. The HJ model gives very good agreement with the DNS. It is also noted that the HGJ-M model predicts better the wall values of the ε_{ij}-components than the original proposal denoted as HGJ, although still not fully reproducing the exact limits. Fig. 9 compares all ε_{ij}-components along the cross-section in the separation bubble. Whereas almost identical values of the ε_{22} and ε_{33} components were obtained by HJ model at the wall distance corresponding roughly to the step height (as a consequence of using the Rotta's high-Reynolds-number limits in the HJ model), the non-linear model formulation by Hallbäck et al. captured the dissipation anisotropy in good agreement with the DNS data.

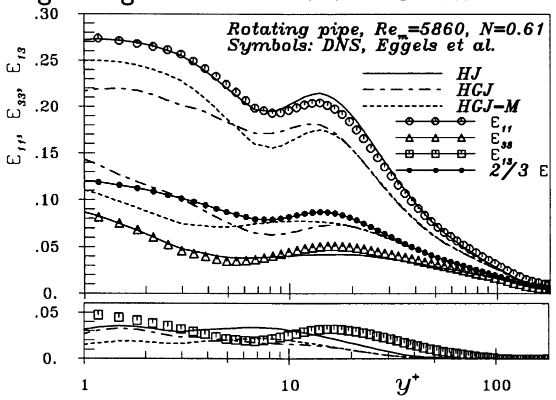

Fig. 8 Axially rotating pipe flow: HJ and HGJ models

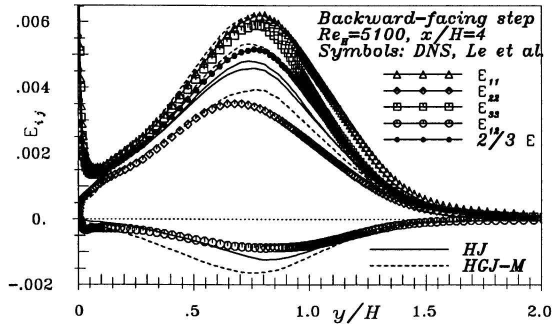

Fig. 9 Backward-facing step flow: HJ and HGJ models at $x/H = 4$ within the separation bubble

CONCLUSIONS

A priori validation of key terms in several algebraic and differential stress models (ASM, DSM) were performed using DNS data for three generic flows: in a plane channel, axially rotating pipe and behind a backward facing step. The subject of validation were the coefficients $G^{(n)}$ of the basis tensors $T_{ij}^{(n)}$ in the ASMs, and the pressure-strain and dissipation terms in the DSMs. These a priori tests enable direct verification of specific model approximations, free from possible contamination and compensating errors that might be introduced by k and ε equations. While no conclusion on the best model could be deduced, the test shows merits and shortcomings of various models with respect to each issue considered, enabling thus to be addressed directly, without the contamination of possible imperfections in the scale-providing k, ε or other equations.

REFERENCES

Craft, T.J., Launder, B.E., and Suga, K. (1996): *Int. J. Heat and Fluid Flow*, Vol. 17, pp 108-115

Craft, T.J. (1998): *Int. J. Heat and Fluid Flow*, Vol. 19, No. 5, pp 541-548

Craft, T.J., Kidger, J.W. and Launder, B.E. (2000): *Int. J. Heat and Fluid Flow*, Vol. 21, pp 338-344

Eggels, J.G.M., Boersma, B.J., and Nieuwstadt, F.T.M. (1994): Lab. for Aero- und Hydrodynamics, Delft University of Technology, October

Fu, S., Launder, B.E., Tselepidakis, D.P. (1987): Thermofluids rep. TFD/87/5, UMIST, Manchester

Gatski, T.B. and Speziale, C.G. (1993): *J. Fluid Mech.*, Vol. 254, pp 59-78

Gibson, M.M., Launder, B.E. (1978): *J. Fluid Mech.*, Vol. 86, pp. 491-511

Hallbäck, M., Groth and Johansson, A.V. (1990): *Physics of Fluids*, A2 (10), pp 1859-1866

Hanjalić, K. and Launder, B.E. (1972): *J. Fluid Mech.*, Vol. 52., pt 4., pp. 609-638

Hanjalić, K., Launder, B.E. (1976): *J. Fluid Mech.*, Vol. 74., pt 4, pp. 593-610

Hanjalić K., and Jakirlić S. (1998): *Computers and Fluids*, Vol. 22, No. 2, pp. 137-156

Jakirlić S. and Hanjalić K. (2001): *2nd Int. Symp. on Turbulence and Shear Flow Phenomena*, Stockholm, 27-29 June

Johansson, A.V., Hallbäck M. (1994): *J. Fluid Mech.*, Vol. 269, pp 143-168

Jongen, T., Mompean, G., and Gatski, T.B. (1998): *Physics of Fluids*, Vol. 10, pp 674-684

Jovanović, J., Ye, Q.-Y., Durst, F. (1995): *J. Fluid Mech.*, Vol. 293, pp 321-347

Khodak, A. and Hirsch, C. (1996): *Comp. Fluid Dynamics '96*, pp 690-696. John Wiley & Sons Ltd.

Knoell, J. and Taulbee, D.B. (1999): *Engineering Turbulence Modelling and Measurements 4*, pp 103-112, Elsevier Science Ltd., Oxford, England.

Launder, B.E., Reece, G.J., Rodi, W. (1975): *J. Fluid Mech.*, Vol. 68, pp. 537-566

Launder, B.E., Tselepidakis, D.P. (1993): *Turbulent Shear Flows*, Vol. 8., pp 81-96

Launder, B.E., Li, S.-P. (1994): *Physics of Fluids*, Vol. 6 (2), pp 999-1006

Le, H., Moin, P. and Kim, J. (1997): *J. Fluid Mech.*, Vol. 330, pp 349-374

Mansour, N. N., Kim, J. and Moin, P. (1988): *J. Fluid Mech*, **194**, 15-44

Moser, R.D., Kim, J. and Mansour, N.N. (1999): *Physics of Fluids*, Vol. 11, No. 4, pp 943-945

Orlandi, P., and Ebstein, D. (2000): *Int. J. Heat and Fluid Flow*, Vol. 21, No. 5, pp. 499-505

Pope, S.B. (1975): *J. Fluid Mech.*, Vol. 72, pp 331-340

Shih, T.H., Lumley, J.L. (1985): Rep. FDA-85-3, Sibley School, Cornell University

Ristorcelli, R., Lumley, J. and Abid (1995): *J. Fluid Mech.*, Vol. 292, pp. 111-152

Rivlin, R.S. and Ericksen, J.S. (1955): *J. Rational Mech. and Analysis*, Vol. 4, pp 323-343

Speziale, C.G., Sarkar, S., and Gatski, T.B. (1991): *J. Fluid Mech.*, Vol. 227, pp. 245-272

Wallin, S. and Johansson, A.V. (2000): *J. Fluid Mech.*, Vol. 403, pp 89-132